Research Article

Impact of Crosstalk Channel Estimation on the DSM Performance for DSL Networks

Neiva Lindqvist,[1,2] Fredrik Lindqvist,[2,3] Marcio Monteiro,[1] Boris Dortschy,[3] Evaldo Pelaes,[1] and Aldebaro Klautau[1]

[1] *Signal Processing Laboratory (LaPS), Federal University of Para, 66075-110 Belem, PA, Brazil*
[2] *Department of Electrical and Information Technology, Lund University, 22100 Lund, Sweden*
[3] *Ericsson Research, Broadband Technologies, Ericsson AB, 16480 Stockholm, Sweden*

Correspondence should be addressed to Neiva Lindqvist, mneiva@ufpa.br

The development and assessment of spectrum management methods for the copper access network are usually conducted under the assumption of accurate channel information. Acquiring such information implies, in practice, estimation of the crosstalk coupling functions between the twisted-pair lines in the access network. This type of estimation is not supported or required by current digital subscriber line (DSL) standards. In this work, we investigate the impact of the inaccuracies in crosstalk estimation on the performance of dynamic spectrum management (DSM) algorithms. A recently proposed crosstalk channel estimator is considered and a statistical sensitivity analysis is conducted to investigate the effects of the crosstalk estimation error on the bitloading and on the achievable data rate for a transmission line. The DSM performance is then evaluated based on the achievable data rates obtained through experiments with DSL setups and computer simulations. Since these experiments assume network scenarios consisting of real twisted-pair cables, both crosstalk channel estimates and measurements (for a reference comparison) are considered. The results indicate that the error introduced by the adopted estimation procedure does not compromise the performance of the DSM techniques, that is, the considered crosstalk channel estimator provides enough means for a practical implementation of DSM.

1. Introduction

High-speed communication over digital subscriber lines (DSLs) can be severely limited by interference from adjacent copper twisted-pair lines in the access network. This destructive crosstalk between neighboring systems is considered as one of the most dominant impairments and consequently poses a limit for performance improvements [1, 2].

Dynamic spectrum management (DSM) is a promising resource management approach to optimize the transmission and improve the data throughput of DSL networks. In summary, DSM is based on improving the spectral utilization by adapting the transmit signals to the slow time-variable channel conditions. Moreover, DSM algorithms exploit multiuser cooperation in order to mitigate or cancel multiuser interference [3–8]. The DSM techniques are commonly organized into three levels depending on the amount of multiuser coordination [5, 7]. For DSM level 1

[9], no crosstalk coupling information is used to optimize the DSL network performance. In DSM level 2 [10–14], the magnitude of the direct and the crosstalk transfer functions are used in order to mitigate the crosstalk. For DSM level 3 (Vectoring), which employs crosstalk cancellation, the crosstalk channel phase information is also required [15–17].

The acquisition of information about the crosstalk channels in the network is usually a demanding task, which may require additional measurement apparatus that are costly to deploy [18]. In, for example, [19–21], different crosstalk estimation solutions have been proposed. However, up to now, the standardization bodies have not yet defined any DSL standard with specific support to estimate the coupling relation between the twisted pairs in a cable binder. With off-the-shelf modems not offering a specific method for estimating the crosstalk channels, various DSM algorithms have been developed and evaluated assuming perfect crosstalk channel information [3, 7, 10, 12]. Moreover, these evaluations adopt
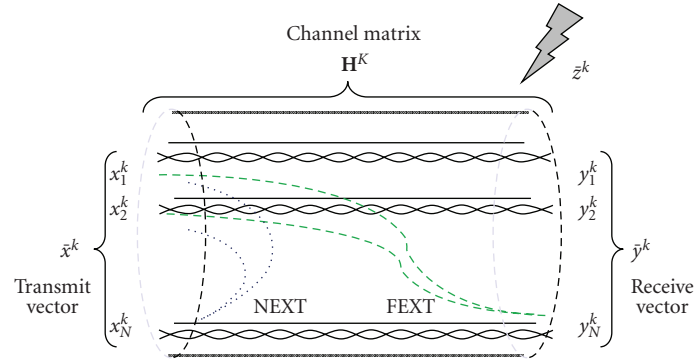
FIGURE 1: Illustration of DMT transmission and occurring NEXT and FEXT interference on a copper access binder.

standardized channel models, which are typically based on statistics and reflect a worst-case scenario [1, 22, 23].

A practical implementation of DSM levels 2 and 3 algorithms must cope with eventual inaccuracies in the crosstalk channel estimation. This is also valid for the stage when evaluating DSM algorithms through computer simulations. Motivated by this fact, the present work investigates the impact of nonideal crosstalk channel estimation on the DSM performance. For this purpose, the crosstalk channel estimator in [24] is considered, since it is a standard-compliant method and does not require costly DSL hardware/software changes or dedicated measurement apparatus for deployment.

A statistical sensitivity analysis is provided to gain insight of how the crosstalk estimation error affects the frequency-dependent bitloading and the resulting data rate for a transmission line, under the exposure of different background noise levels. It is worth to notice that, in general, the level 2 DSM algorithms are formulated in order to optimize the *bitloading*, or equivalently the *power loading*, and generate a solution for the spectrum management problem (see, e.g., [25]).

Since the presence of the crosstalk estimation error impacts the final solution of the DSM algorithms, the DSM performance is evaluated based on the achievable data rates obtained through DSL network simulations. For these simulations, network scenarios consisting of real twisted-pair cables are considered and in addition, both crosstalk-channel estimates and references measurements are used for the comparison. The crosstalk channel reference measurements are conducted in a laboratory using a network analyzer and ordinary twisted-pair cables. For each scenario, three state-of-the-art DSM algorithms are simulated and the results in terms of achievable data rate region curves are analyzed.

The remainder of this work is organized as follows. Section 2 presents the system model and defines the notation. Section 3 describes the principles of the power spectrum density (PSD) level optimization applied by DSM algorithms as a solution to the spectrum management problem. In Section 4, the employed crosstalk channel estimation is introduced. Section 5 is dedicated to the proposed statistical sensitivity analysis. Details about the network scenarios, laboratory setup and obtained measurements are given in Section 6. The DSM performance evaluation

assuming the crosstalk channel estimation is presented in Section 7. Finally, a summary and conclusions are provided in Section 8.

2. System Model

Traditionally, DSL broadband access networks have been analyzed from a single-user system perspective. However, for DSM-enabled systems, such as the ones considered here, the DSL lines are used in a multiuser context. This perspective requires a multiuser or a multiple-input multiple-output (MIMO) channel model (this should not be confused with the concept of MIMO or vectoring DSM, related to DSM level 3 algorithms [3, 15]), which permits the joint-user coordination concept utilized by the DSM techniques.

In this work, DSM algorithms are applied on a copper access binder, which consists of N users (i.e., lines) equipped with DSL transceivers. Each transceiver employs discrete multitone modulation (DMT) and operates over a twisted-pair line with K independent and parallel subchannels (tones) over the frequency band plan [1]. This means that the received signal vector on tone k can be modeled as [1, 5]

$$\bar{y}^k = \mathbf{H}^k \bar{x}^k + \bar{z}^k, \quad \text{for } k = 1, 2, \ldots, K, \quad (1)$$

where

(i) $\bar{x}^k = [x_1^k, x_2^k, \ldots, x_N^k]^T$ is the transmitted signal vector on tone k for all N users;

(ii) $\bar{y}^k = [y_1^k, y_2^k, \ldots, y_N^k]^T$ is the received signal vector on tone k for all N users;

(iii) $\bar{z}^k = [z_1^k, z_2^k, \ldots, z_N^k]^T$ is the additive noise vector on tone k including the extrinsic network impairment, for example, impulse noise, radio frequency interference (RFI), thermal noise and alien crosstalk [1],

(iv) $\mathbf{H}^k$ corresponds to an $N \times N$ matrix containing the channel transfer functions on tone k.

The DMT transmission for tone k in a cable binder, represented by (1), is illustrated in Figure 1. Basically two types of crosstalk are present in the DSL network: the far-end (FEXT) and the near-end (NEXT) crosstalks, shown in Figure 1. By assuming only frequency division duplex DMT transmission, where upstream and downstream frequency
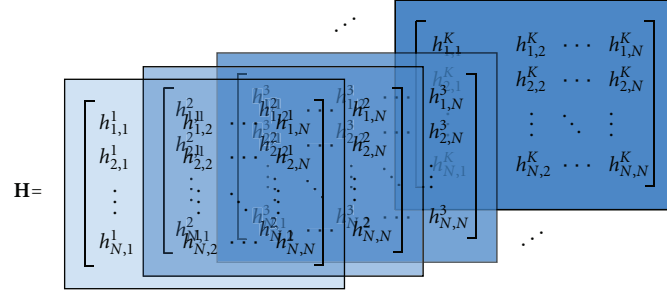
FIGURE 2: MIMO channel matrix $\mathbf{H}$ of dimension $N \times N \times K$.

bands are nonoverlapping, it is reasonable to neglect the weak NEXT influence [1]. The channel matrix $\mathbf{H}$ characterizes the binder by representing both the direct and the FEXT coupling transfer functions, and can be interpreted along the three dimensions $N \times N \times K$, as illustrated in Figure 2.

Each channel vector $\overline{h}_{n,m} = [h_{n,m}^1, h_{n,m}^2, \ldots, h_{n,m}^K]^T$ represents the transfer function of the channel from transmitter m to receiver n, over the tones. For the case where $m = n$, the diagonal vectors $\overline{h}_{1,1}, \overline{h}_{2,2}, \ldots, \overline{h}_{N,N}$ correspond to the direct transfer functions of the twisted-pair lines. Similarly, the off-diagonal vectors $\overline{h}_{n,m}$, for $n \neq m$, correspond to the FEXT transfer functions between the lines.

3. PSD Level Optimization and the Spectrum Management Problem

DSM levels 1 and 2 employ PSD level optimization aiming to assign a transmit PSD for each user, within the DSL network, in order to minimize the crosstalk interference. The PSD assignment is conducted according to a set of predefined criteria and constraints, for example, maximize the user rates under power limitation. For the nth user, the PSD of the transmitted signal on tone k is here defined by $E\{|x_n^k|^2\}$, whose maximum value is specified by the DSL standard(s), $E\{\cdot\}$ denotes the statistical mean value. Hence the transmit power on tone k for user n can be expressed as $s_n^k = \Delta_f E\{|x_n^k|^2\}$, where Δ_f is the tone frequency spacing. The transmit power vector with K tones for user n can be represented by $\overline{s}_n = [s_n^1, s_n^2, \ldots, s_n^K]^T$.

The PSD level optimization allows the transmitter to adaptively vary the number of transmitted bits per tone according to the characteristics of the channel. This practice avoids the use of fixed transmit PSDs for all users and thereby prevents a loss in performance [5, 7]. The final result of the PSD level optimization is a dynamic shaping of the transmit PSDs according to the interference levels within the used frequency band. In practice, the PSD dynamic shaping is made possible by the bitloading concept utilized by DMT [1]. This allocation of bits per tone is performed for each subchannel and can be expressed as follows:

$$b_n^k = \log_2 \left[1 + \frac{s_n^k |h_{n,n}^k|^2}{\Gamma \left(\sigma_{k,n}^2 + \sum_{m \neq n} s_m^k |h_{n,m}^k|^2 \right)} \right], \quad (2)$$

where

(i) b_n^k is the achievable bitloading on tone k for user n;

(ii) $\sigma_{k,n}^2$ is defined as $\Delta_f E\{|z_n^k|^2\}$ and represents the additive noise power, that is, the background noise level, on tone k at receiver n, which coincides with the noise variance given that $E\{|z_n^k|\} = 0$. It is assumed that $\sigma_{k,n}^2$ contains the thermal noise, alien crosstalk, and radio frequency interference;

(iii) Γ denotes the signal-to-noise (SNR) ratio *gap*, which is a function of the desired bit error rate (BER). The *gap* is an indicator of how closely the bit rate comes to the theoretical channel capacity [1, 2].

Considering that each transceiver (modem) treats the interference from the other transceivers as noise, the achievable bit rate of user n can be formulated as [1, 2]

$$R_n = f_{\text{sym}} \sum_{k=1}^K b_n^k, \quad (3)$$

where f_{sym} represents the symbol rate of the DMT transceivers [5]. Similarly, the total power assigned to the nth user can be expressed as

$$P_n = \sum_{k=1}^K s_n^k. \quad (4)$$

The total data throughput is an often used performance measure for communication networks. In the context of DSM, we can assume that the optimization of a multiuser DMT (multicarrier) system corresponds to the problem of maximizing the total throughput subject to system resource-constraints. Thus, the spectrum management problem is commonly formulated as a maximization problem of the weighted sum rate, subject to a power constraint per user. That is,

$$\text{maximize} \quad \sum_{n=1}^N \omega_n R_n$$

$$\text{subject to} \quad \sum_{k=1}^K s_n^k \leqslant P_n^{\max}, \quad n = 1, 2, \ldots, N, \ s_n^k \geq 0, \quad (5)$$

where ω_n is the nonnegative constant for user n that provides different priorities (or weights) for users and $P_n^{\max}$ is the maximum available power for user n.

The optimization problem represented by (5) can be interpreted as a search to find a set of nonnegative s_n^k values, under a tradeoff between maximizing the data rate R_n and avoiding crosstalk interference. Generally, in the context of a solution for the spectrum management problem, the DSM algorithms aim to find the optimum values for the transmit power allocation (power loading) s_n^k, which is equivalent to find the optimum values for the bit allocation (bitloading) b_n^k, both for $n = 1, 2, \ldots, N$ and for $k = 1, 2, \ldots, K$.

In this work, the DSM algorithms in [10, 12] formulated to solve the weighted sum-rate maximization problems (rate adaptive) are considered. Therefore, the sensitivity analysis performed in the forthcoming section is based on the bitloading formulation. However, this analysis could also be cast in a power loading framework without loss of generality, due to the equivalence of the rate and power adaptive problems [25].

4. Crosstalk Channel Estimation

The DSM level 2 compliant algorithms used in this work provide a solution to the spectrum management problem formulated in (5). These algorithms require channel information about the square magnitude of the direct and crosstalk channels. As previously mentioned, the corresponding channel phase information can be neglected for DSM level 2 applications. The channel matrix $\mathbf{H}$, introduced in Section 2, characterizes the access cable binder and contains the direct and the FEXT transfer functions. It can be presumed that the direct transfer functions are known a priori, since the procedures to obtain them are supported by the current DSL standards [26].

In this work, the square magnitude of the off-diagonal elements of channel matrix $\mathbf{H}$ is obtained by the crosstalk channel estimation procedure described in [24]. Since the transmitted PSD for each user is assumed known, the total received crosstalk can be calculated from the crosstalk channel estimates. Thus, throughout the paper we define the method proposed in [24] as the *Crosstalk Estimator*, where no a priori channel information is used.

In the following subsection a brief summary of the *Crosstalk Estimator* is given with focus on the behavior of the estimation error [24]. This provides the fundamental understanding of the error to expect when estimating the FEXT with the employed estimator. This is further elaborated on in Section 5, where a statistical sensitivity analysis of the achievable bitloading and data rate is presented.

4.1. Crosstalk Channel Estimation Error. The *Crosstalk Estimator* presented in [24] relies only on standardized DSL signals and protocols, for example, the two-port measurement procedure referred to as Loop Diagnostic [26], which are supported by off-the-shelf DSL modems that are DSL standard compliant. More specifically, the estimator is based on sequential PSD measurements at the far-end side of

the lines with only one near-end transmitter active per measurement sequence. The procedure is typically executed and coordinated from a network management system with independent processing among the far-end receivers. It should be emphasized that the FEXT channel estimation has to be performed only once, or seldom, since the FEXT channels do not (normally) vary significantly over time.

The sequential PSD-based estimate of the FEXT channel attenuation $|h_{n,m}^k|^2$ can be formulated as [24]

$$\widetilde{\left| h_{n,m}^k \right|}^2 = \frac{P_y^k - P_z^k}{P_x^k}, \tag{6}$$

where P_x^k, P_y^k, and P_z^k are the transmit PSD on line m, the receive FEXT PSD on line n, and the additive noise PSD on line n, respectively, for tone k and in unit Watts. In practice, however, the PSD measurements retrieved via the Loop Diagnostic protocol are not error-free due to the fact that, for example, the PSD measurements are quantized and, in combination with the additive noise, fluctuate in discrete steps around the mean values. That is, for tone k, the obtained PSD measurements can be expressed as

$$\hat{P}_{\mathrm{dBm/Hz}}^k = P_{\mathrm{dBm/Hz}}^k + \Delta_{\mathrm{dBm/Hz}}, \tag{7}$$

where $P_{\mathrm{dBm/Hz}}^k$ denotes the nonquantized PSD and $\Delta_{\mathrm{dBm/Hz}}$ is the quantized measurement error modeled as a discrete integer-valued random variable with uniform distribution, that is, $\Delta_{\mathrm{dBm/Hz}} \in \{-\delta, \delta + 1, \ldots, 0, \ldots, \delta\}$ dBm/Hz. The PSD measurements are converted to unit Watts according to

$$P = 10^{(P_{\mathrm{dBm/Hz}}^k - 30)/10} B, \tag{8}$$

where B is the measurement bandwidth in Hz. It is known from the experiments in [24] that it is reasonable to consider δ as typically varying in the range of 1 to 3 dBm/Hz, independently of the magnitude of the measured PSD. Moreover, for the case where the measured FEXT is much larger than the background noise level, that is, $P_y \gg P_z$, the measurement error associated with P_z has essentially no impact when compared to the measurement error of P_y. Consequently, the measurement error of P_z can be neglected. Based on these assumptions, the obtained FEXT channel estimate can straightforwardly be derived from (6)–(8) and yields

$$\widetilde{\left| h_{n,m}^k \right|}^2 = \frac{P_y^k \Delta - P_z^k}{P_x^k}, \tag{9}$$

where both the FEXT channel estimate given by (9) and the measurement error Δ are in linear scale.

The resulting FEXT channel estimation error in dB, denoted by $\widetilde{\Delta}_{\mathrm{dB}}$, can be defined as the ratio between (6) and (9), that is,

$$\widetilde{\Delta}_{\mathrm{dB}} = 10 \log_{10} \left(\frac{1 - P_z/P_y}{\Delta - P_z/P_y} \right), \tag{10}$$

which shows that the PSD measurement error Δ affects the FEXT channel estimate in a nonlinear way. It should be

noticed the difference between the *PSD measurement error* Δ and the *FEXT channel estimation error* $\widetilde{\Delta}$.

Under the given assumption that $P_y \gg P_z$, the estimation error in (10) yields

$$\widetilde{\Delta}_{\text{dB}} \approx 10 \log_{10} \frac{1}{\Delta}. \tag{11}$$

Equation (11) indicates that the estimation error $\widetilde{\Delta}_{\text{dB}}$ has an approximative linear dependence on the PSD measurement error Δ (in logarithmic scale) when $P_y \gg P_z$. The experimental results in [24] suggests that the linear error approximation is reasonable if the difference between P_y and P_z corresponds to at least 5 dB, in which case the estimation error $\widetilde{\Delta}_{\text{dB}}$ is typically confined to the interval $[-3, 3]$ dB. Hence, in line with [24] this work assumes an FEXT channel estimation error uniformly distributed within $[-3, 3]$ dB.

5. Statistical Sensitivity Analysis

This section provides a statistical sensitivity analysis of the achievable bitloading, represented by (2), in function of the FEXT channel estimation error parameter $\widetilde{\Delta}$. The purpose of this analysis is to gain insight of how the bitloading and the data rate are affected by the FEXT channel estimation error.

Firstly, the probability density function (PDF) of the bitloading b_n^k, for line n and tone k, is derived given that the FEXT channel estimation error is modeled as a uniform random variable according to Section 4.1. Secondly, we derive the PDF of the data rate achieved on line n, resulting from the uniformly distributed estimation error. Thirdly, numerical results for the above mentioned PDFs are presented based on measured FEXT couplings of an ordinary twisted-pair cable.

5.1. Deriving the PDF of b_n^k. The relation between the bitloading and the crosstalk estimation error $\widetilde{\Delta}$ reveals a variation in the assignment of bits per tone caused by the nonperfect crosstalk channel estimation. Such variation in the number of bits is also reflected in the final solutions of the DSM algorithms in terms of a spread in the achievable data rate, given by (3). Motivated by this fact, the PDF of b_n^k in function of the random variable $\widetilde{\Delta}$ is derived in the sequel while the PDF of the data rate is derived in Section 5.2.

We start out defining the relation between the bitloading b_n^k and the crosstalk estimation error $\widetilde{\Delta}$ by reformulating the expression in (2) as

$$b_n^k = \log_2 \left[1 + \frac{s_n^k \left| h_{n,n}^k \right|^2}{\Gamma \left(\sigma_{k,n}^2 + \sum_{m \neq n} s_m^k \widetilde{\Delta} \left| h_{n,m}^k \right|^2 \right)} \right]. \tag{12}$$

It can be noted that the estimation error parameter $\widetilde{\Delta}$ appears in (12) as a factor that multiplies with $|h_{n,m}^k|^2$, where the latter corresponds to the FEXT channel attenuation between lines m and n.

For convenience, we also define the following nonnegative quantities:

$$A = \frac{s_n^k \left| h_{n,n}^k \right|^2}{\Gamma}, \qquad B = \sum_{m \neq n} s_m^k \left| h_{n,m}^k \right|^2. \tag{13}$$

With the help of these two constants, b_n^k can be written as a function $g(\widetilde{\Delta})$ according to

$$b_n^k = g\left(\widetilde{\Delta}\right) = \log_2 \left[1 + \frac{A}{\sigma_{k,n}^2 + \widetilde{\Delta} B} \right]. \tag{14}$$

By defining the inverse function $g^{-1}(b_n^k)$, the parameter $\widetilde{\Delta}$ can be expressed as

$$\widetilde{\Delta} = g^{-1}\left(b_n^k\right) = \frac{A - \sigma_{k,n}^2 \left(2^{b_n^k} - 1\right)}{B\left(2^{b_n^k} - 1\right)}. \tag{15}$$

Thus, the PDF of b_n^k, denoted by $f_{b_n^k}(b_n^k)$, can be formulated as [27]

$$f_{b_n^k}\left(b_n^k\right) = \left| \frac{\partial\left(g^{-1}\left(b_n^k\right)\right)}{\partial b_n^k} \right| f_{\widetilde{\Delta}}\left(g^{-1}\left(b_n^k\right)\right), \tag{16}$$

where $f_{\widetilde{\Delta}}$ is the PDF of $\widetilde{\Delta}$ and the derivative of $g^{-1}(b_n^k)$ is

$$\frac{\partial\left(g^{-1}\left(b_n^k\right)\right)}{\partial b_n^k} = \frac{-A 2^{b_n^k} \ln 2}{B\left(2^{b_n^k} - 1\right)^2}. \tag{17}$$

Hereafter the PDF of $\widetilde{\Delta}$ (in linear scale) is determined. In line with [24], we assume that the measurement error $\widetilde{\Delta}_{\text{dB}}$ is uniformly distributed (in unit dB), that is,

$$f_{\widetilde{\Delta}_{\text{dB}}}\left(\widetilde{\Delta}_{\text{dB}}\right) = \begin{cases} 0, & \widetilde{\Delta}_{\text{dB}} < c_1, \\ \dfrac{1}{(c_2 - c_1)}, & c_1 \leq \widetilde{\Delta}_{\text{dB}} \leq c_2, \\ 0, & \widetilde{\Delta}_{\text{dB}} > c_2, \end{cases} \tag{18}$$

where c_1 and c_2 are constants in dB. It now follows directly from (18) that the PDF of $\widetilde{\Delta}$ yields

$$f_{\widetilde{\Delta}}\left(\widetilde{\Delta}\right) = \begin{cases} 0, & \widetilde{\Delta} < 10^{c_1/10}, \\ \left| \dfrac{10}{\widetilde{\Delta} \ln 10} \right| \cdot \dfrac{1}{(c_2 - c_1)}, & 10^{c_1/10} \leq \widetilde{\Delta} \leq 10^{c_2/10}, \\ 0, & \widetilde{\Delta} > 10^{c_2/10}. \end{cases} \tag{19}$$

Thus, from the combination of (16)–(19), it follows that the PDF of b_n^k can be expressed as

$$f_{b_n^k}\left(b_n^k\right) = \begin{cases} 0, & b_n^k < \gamma_2, \\ \dfrac{A 2^{b_n^k} 10 \ln 10}{(c_2 - c_1)\left(2^{b_n^k} - 1\right) \mathcal{W}}, & \gamma_2 \leq b_n^k \leq \gamma_1, \\ 0, & b_n^k > \gamma_1, \end{cases} \tag{20}$$

as $\mathcal{W}$ denotes $[A - \sigma_{k,n}^2(2^{b_n^k} - 1)]$, and

$$\gamma_1 = \log_2\left[1 + \frac{A}{\sigma_{k,n}^2 + 10^{c_1/10}B}\right],$$

$$\gamma_2 = \log_2\left[1 + \frac{A}{\sigma_{k,n}^2 + 10^{c_2/10}B}\right]. \tag{21}$$

Finally, by replacing A and B in expression (20) according to (13), the PDF of b_n^k is obtained in the form

$$f_{b_n^k}\left(b_n^k\right) = \begin{cases} 0, & b_n^k < \gamma_2, \\ \dfrac{s_n^k\left|h_{n,n}^k\right|^2 2^{b_n^k} 10 \ln 10}{(c_2 - c_1)\left(2^{b_n^k} - 1\right)\hbar}, & \gamma_2 \le b_n^k \le \gamma_1, \\ 0, & b_n^k > \gamma_1, \end{cases} \tag{22}$$

as $\hbar$ denotes $[s_n^k|h_{n,n}^k|^2 - \Gamma\sigma_{k,n}^2(2^{b_n^k} - 1)]$, and

$$\gamma_1 = \log_2\left[1 + \frac{s_n^k\left|h_{n,n}^k\right|^2}{\Gamma\left(\sigma_{k,n}^2 + 10^{c_1/10}\sum_{m \neq n} s_m^k\left|h_{n,m}^k\right|^2\right)}\right], \tag{23}$$

$$\gamma_2 = \log_2\left[1 + \frac{s_n^k\left|h_{n,n}^k\right|^2}{\Gamma\left(\sigma_{k,n}^2 + 10^{c_2/10}\sum_{m \neq n} s_m^k\left|h_{n,m}^k\right|^2\right)}\right]. \tag{24}$$

The PDF $f_{b_n^k}(b_n^k)$ in (22) represents the variation of the number of bits for tone k and line n due to the presence of the crosstalk estimation error $\widetilde{\Delta}$ through the constants c_1 and c_2. The interval for the number of bits assigned per tone, that is, the interval of existence of the PDF, is limited by γ_1 and γ_2 defined in (23) and (24), respectively. It can be noted from (22) that the shape of the PDF does not depend on the FEXT crosstalk channel values, that is, $|h_{n,m}^k|^2$ for $m \neq n$, which are present only in the definition of γ_1 and γ_2.

5.2. Deriving the PDF of R_n. In the previous subsection the PDF $f_{b_n^k}(b_n^k)$ was derived in order to gain insight of the variation in the number of allocated bits (per tone) due to the presence of $\widetilde{\Delta}$. In the following, the variation in the data rate R_n achieved by a line n in function of the crosstalk estimation error $\widetilde{\Delta}$ is analyzed through the derivation of the PDF of the data rate R_n, denoted by $f_{R_n}(R_n)$.

The achievable data rate for an user n, as introduced in (3), can be reformulated according to (12) as

$$R_n = f_{\text{sym}}\sum_{k=1}^K b_n^k$$

$$= f_{\text{sym}}\sum_{k=1}^K \log_2\left[1 + \frac{s_n^k\left|h_{n,n}^k\right|^2}{\Gamma\left(\sigma_{k,n}^2 + \sum_{m \neq n} s_m^k\widetilde{\Delta}\left|h_{n,m}^k\right|^2\right)}\right]. \tag{25}$$

Hence the PDF of the data rate $f_{R_n}(R_n)$ is obtained as

$$f_{R_n}(R_n) = f_{\text{sym}}\left[f_{b_n^k}(b_n^1) \otimes f_{b_n^k}(b_n^2) \otimes \cdots \otimes f_{b_n^k}\left(b_n^K\right)\right], \tag{26}$$
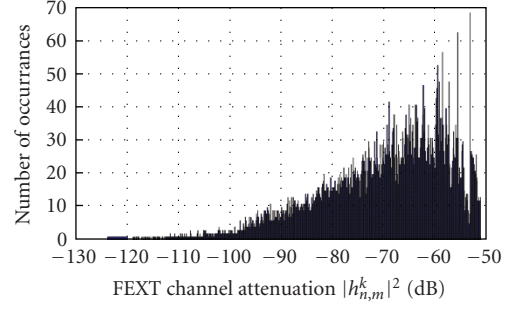

FIGURE 3: Histogram of the measured FEXT channel attenuation $|h_{n,m}^k|^2$ for an ordinary 500 m long 26 AWG cable of 20 twisted pairs and assuming downstream ADSL2+ frequency bandplan.

where $\otimes$ denotes the convolution operator. Instead of performing the cumbersome repeated convolutions, we resort to the Central Limit Theorem (CLT) [27], given that R_n is a sum of random variables. It should be noted that b_n^k for $k = 1, \ldots, K$ are in general not i.i.d. variables since the PDF $f_{b_n^k}(b_n^k)$ is determined by the frequency-dependent properties of the cable binder, the background noise, and so forth as seen in (22). However, it is well known that the CLT often (approximately) applies for non i.i.d. cases as the number of random variables goes to infinity. The results in Section 5.3 confirm that the PDF $f_{R_n}(R_n)$ is approximately Gaussian for our test case, that is, for the cable binder and system considered. Thus, the PDF of the data rate can be approximated by the Gaussian PDF
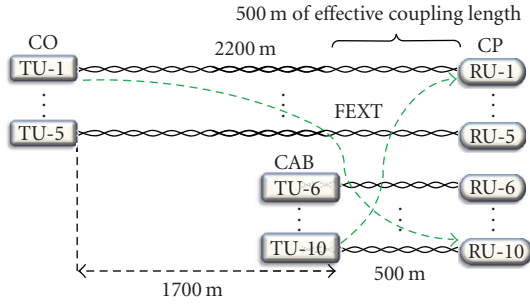
$$f_{R_n}(R_n) = f_{\text{sym}}\frac{1}{\sqrt{2\pi\sigma_{R_n}^2}}e^{-(R_n - E\{R_n\})^2/2\sigma_{R_n}^2}, \tag{27}$$

where the mean $E\{R_n\}$ and the variance $\sigma_{R_n}^2$ are obtained as

$$E\{R_n\} = f_{\text{sym}}\sum_{k=1}^K E\left\{b_n^k\right\}, \qquad \sigma_{R_n}^2 = f_{\text{sym}}^2\sum_{k=1}^K \sigma_{b_n^k}^2. \tag{28}$$

5.3. Numerical Results. The FEXT coupling functions measured on $N = 20$ twisted pairs of an ordinary 500 m long (26 AWG) telephone cable are considered for our study case. Since the knowledge of the FEXT distribution behavior is helpful in understanding the forthcoming results, the histogram of the measured attenuation values $|h_{n,m}^k|^2$ for tone $k = 33, 34, \ldots, K$, and line $n = 1, 2, \ldots, N$, is shown in Figure 3, assuming the ADSL2+ downstream frequency bandplan [26], where $K = 512$. From Figure 3 we note that the majority of the values $|h_{n,m}^k|^2$ are within the interval from -50 dB to -80 dB. This reflects a typical behavior of the crosstalk channels for such cable type and length. Thus, given a transmit PSD of -40 dBm/Hz [26], the received FEXT levels are mainly within -90 dBm/Hz to -120 dBm/Hz.

In the following we consider a specific transmission line $n = 1$ among the $N = 20$ twisted pairs of the 500 m cable (26 AWG), an SNR-gap Γ of 12.8 dB, and a frequency-flat transmit PSD set to -40 dBm/Hz for all the ADSL2+ modems. Figure 4 demonstrates an application of

FIGURE 4: The PDF $f_{b_n^k}(b_n^k)$ for a tone $k = 300$ and for different background noise $\sigma_{k,n}^2$ levels. The bitloading calculated with (2), corresponding to error-free estimation ($\widetilde{\Delta} = 1$), is represented by the vertical lines.

(22) for an arbitrary tone $k = 300$ and line $n = 1$ of our cable binder. Here, for different background noise levels, the corresponding PDF $f_{b_n^k}(b_1^{300})$ given by (22) is compared with the achievable number of bits b_n^k calculated using (2), where the latter are indicated by the vertical lines. Under the described conditions, it can be observed that for low background noise levels, that is, when the channel is mainly crosstalk-limited, the PDF of $f_{b_n^k}(b_1^{300})$ is approximately uniformly distributed. However, a change in the PDF shape occurs if the background noise level is greater than (roughly) $-100\,$dBm/Hz, since the channel then also becomes background noise limited, resulting in that the PDF $f_{b_n^k}(b_1^{300})$ tends to be nonuniformly distributed.

The PDF $f_{R_n}(R_n)$ in (27) for transmission line $n = 1$ is shown in Figure 5 with red dashed lines for different background noise $\sigma_{k,n}^2$ levels. The corresponding Monte Carlo simulations, for each background noise level, is also shown according to the figure legend. In addition, the data rate calculated with (3), which corresponds to $\widetilde{\Delta} = 1$ ($\widetilde{\Delta}_{\mathrm{dB}} = 0$), is depicted in Figure 5 by the vertical lines.

If a comparison is made between the PDFs calculated with (27) and the corresponding Monte Carlo simulations, it is clear from Figure 5 that the CLT applies and that the PDF can be considered Gaussian, for our study case. Furthermore, according to Figure 5, the maximum spread in the data rate caused by $\widetilde{\Delta}$ is approximately 400 kbps, for the considered background noise levels. This corresponds to an uncertainty of less than 2% of the mean data rate for the considered line. Moreover, the PDF $f_{R_n}(R_n)$ becomes slightly biased as the $\sigma_{k,n}^2$ level increases, in the sense that the mean value $E\{R_n\}$ does not correspond (exactly) to the case, where $\widetilde{\Delta} = 1$.

FIGURE 5: The PDF $f_{R_n}(R_n)$ for a transmission line $n = 1$, and for different background noise levels, are depicted by the dashed red lines. The curves following the figure legend are the corresponding Monte Carlo simulations. The data rates calculated with (3), are represented by the vertical lines.

FIGURE 6: Access network *Scenario I*.

This corresponds to a scenario which is not only limited by the crosstalk; whereas the assumed uniform error model of the *Crosstalk Estimator* is no longer valid as described in Section 4.1.

6. Laboratory Setup for DSM Simulations

This section describes the laboratory setup utilized to obtain the two network scenarios and their respective channel measurements and estimates, which are used during the DSM simulations. The used access network *Scenario I* and *Scenario II* are depicted in Figures 6 and 7, respectively. Both networks comprise transmitter units (TUs) located at the central office (CO) and at the cabinet (CAB) side. The receiver units (RUs) are located at the customer premises (CPs) side. All considered DSL transceiver units correspond to ADSL2+ modems [26]. The access binder in Figures 6 and 7 is built up with real twisted-pair cables consisting of 0.40 mm (26 AWG) copper lines of lengths 500 m, 1500 m, and 2200 m.

For the purpose of establishing a reference, a network analyzer (NA) is used to measure the "ideal" square magnitude of the FEXT channels. This measurement is performed by connecting the NA equipment directly to the cable ends,

FIGURE 7: Access network *Scenario II*.

- —— FEXT model
- - - - NA measurement
- —— Crosstalk estimator (processed data)
- -•- Crosstalk estimator (raw data)

(b)

FIGURE 8: Square-magnitude of the FEXT channels for *Scenario I* representing: the worst-case FEXT model; the NA measurements; the *Crosstalk Estimator* estimates in the form of raw data and smoothed curves with the application of an MA filter.

that is, no DSL modems are involved in the measurement setup. The NA also provides the square magnitude of the direct channels used in the forthcoming DSM performance simulations. The ADSL2+ downstream band from frequency 142.31 kHz to 2.208 MHz is considered and a tone spacing of $\Delta_f = 4.3125$ kHz is employed in order to comply with the DMT tone spacing used for ADSL2+ [26]. Figure 8 shows the square magnitude of the FEXT channels for *Scenario I* obtained with the NA, the *Crosstalk Estimator* [24], and with the so-called 99% worst-case FEXT model [22]. The FEXT model is only used for comparison and is calculated based on the true line length and the measured insertion loss. Similar measurements and estimation results are also obtained for *Scenario II*.

In Figure 8, the estimates acquired with the *Crosstalk Estimator* are presented in the forms of raw data and processed data. The raw data are the primary estimation results and include a small number of missing data points. The missing data occur mainly at the lower frequencies due to the presence of high-pass filters in the transceivers, which in turn attenuates the received signal to the level of the background noise, preventing those channel values to be estimated (see [24] for details). Interpolation and extrapolation are therefore applied in order to recover the missing data and overcome this problem, as shown by the curves representing the processed data in Figure 8. In addition, a moving average (MA) filter is employed to smooth the curves prior to executing the DSM algorithms. Furthermore, it should be noted that the (reference) NA measurements and the FEXT model do not describe the complete FEXT channels seen by the *Crosstalk Estimator*, since the two former quantities do not include the effects of the transceiver filters and the analog front-ends of the DSL modems. Due to this, the obtained NA measurements and the FEXT-model values are compensated with the transceiver characteristics, as described in [24], providing a more fair comparison. The effects of the transceiver-filter compensation is especially noticeable at the frequency-band edges in Figure 8; that is, high-pass and low-pass filtering.

The deviations of the FEXT channel estimates in Figure 8 indicate, as expected, that the FEXT model over estimates the FEXT influence. The *Crosstalk Estimator*, however, is able to follow the shape of the NA measurements quite well. This ability of the estimator is of particular interest for the DSM approach. More specifically, the *Crosstalk Estimator* provides
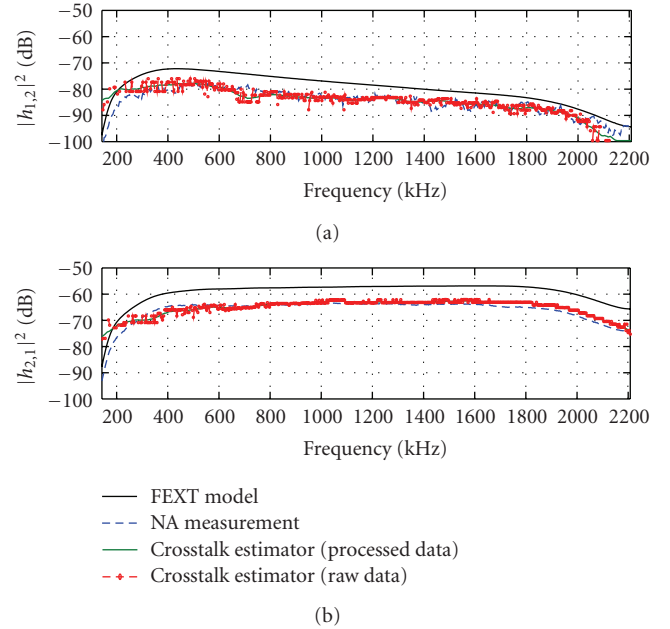
an estimate of the FEXT channels for *Scenarios I* and *II* with a mean deviation less than 3 dB relative to the the NA measurements for most frequencies. Thus, the accuracy of the estimation results is in line with [24].

7. Impact of Crosstalk Channel Estimation on DSM performance

In this section we present a simulation-based investigation of the impact of nonideal FEXT channel estimation on the DSM performance. The *Crosstalk Estimator* described in Section 4 is applied to the two access network scenarios shown in Figures 6 and 7. Based on the obtained estimates of the FEXT channels, we evaluate the performance of the two DSM algorithms *Iterative Spectrum Balancing (ISB)* [10] and *Successive Convex Approximation for Low-complExity (SCALE)* [12].

The DSM simulations utilize the measured direct channel gains and the PSD of the background noise, obtained with a network analyzer (NA) and with the Loop Diagnostic procedure [24, 26], respectively. The simulations further assumes: SNR-gap of 9.8 dB, noise margin of 6 dB, coding gain of 3 dB, BER of 10^{-7}, transmit power for each modem of 19.4 dBm, and a maximum of 15 bits per tone.

7.1. Results for Scenario I. The DSM algorithms are first executed using the FEXT channels provided by the (transceiver-compensated) NA measurements described in the previous section. The so-obtained DSM results are considered as the (true) reference values. Thereafter the DSM algorithms is executed based on the FEXT channels from the *Crosstalk*
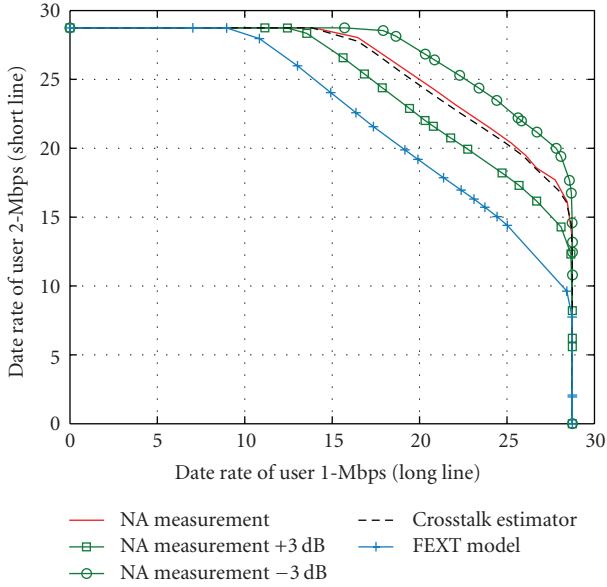
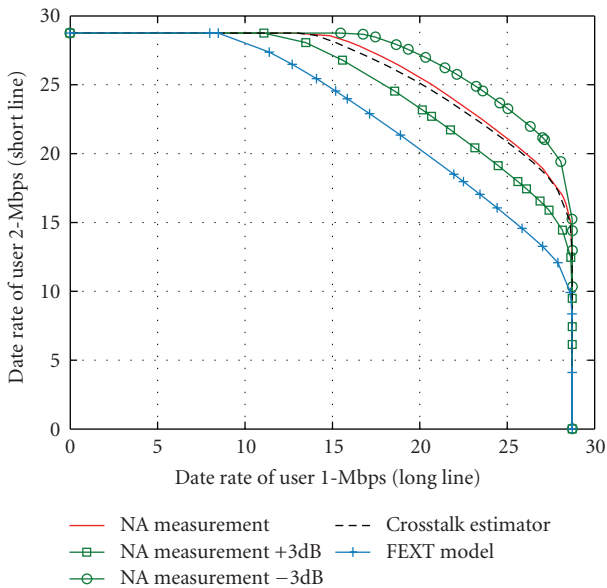FIGURE 9: Simulation results obtained with the ISB algorithm.

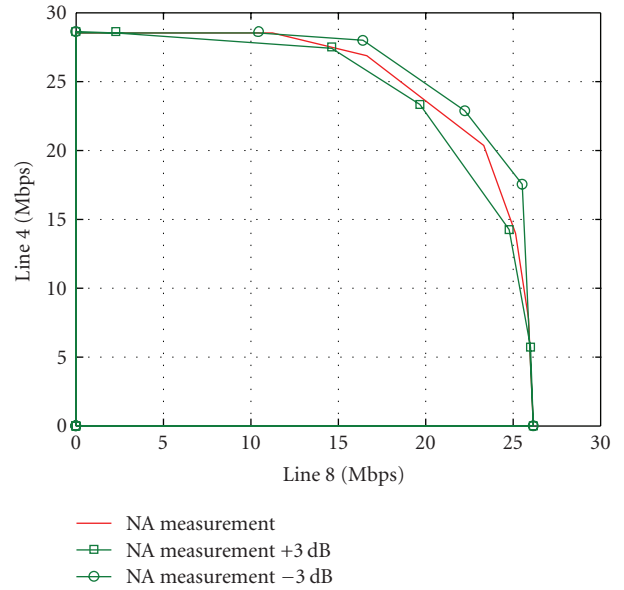FIGURE 10: Simulation results obtained with the SCALE algorithm.

FIGURE 11: Section of the 10-dimensional rate region curve, obtained with SCALE, for 2 users (out of 10 users) with nonequal length lines.

Estimator and from the (transceiver-compensated) FEXT model.

Figures 9 and 10 show the obtained rate regions for the 2-users *Scenario I* (Figure 6) using the DSM algorithms ISB and SCALE. It should be understood that the rate region consists of a set of points representing possible transmission-rate combinations between the two users, where the points belonging to the outermost border-line indicates the maximum achievable data rate calculated according to (3).

The results plotted in Figures 9 and 10 show that for both the ISB and the SCALE algorithms, the FEXT channel estimates are accurate enough to provide values close to the reference (NA measurements) values. That is, the deviation in data rates obtained with the *Crosstalk Estimator* and the

NA measurement are less than 500 kbps. It is worth to notice that this deviation is in the same order as the spread of the data rate found in Section 5.3, even though the scenarios are not the same. The rate region obtained with the FEXT model demonstrates, as expected, that the user data rates are significantly underestimated with the model.

To further investigate the confidence region of data rates achieved with the *Crosstalk Estimator*, the DSM algorithms are once more simulated based on the NA measurements, but now with an assumed error-offset of $+3$ dB or -3 dB for each tone, representing the extreme values of the estimation error. From Figures 9 and 10 it can be noted that the so-obtained confidence region spans roughly data rates from -3 Mbps to $+3$ Mbps relative the reference data rates. It is interesting to note that even though the borders of the confidence regions should correspond to the unlikely worst-case for the *Crosstalk Estimator*, the achieved data rates are still closer to the reference values than the rates obtained with the FEXT model.

7.2. Results for Scenario II. The 10 users *Scenario II* depicted in Figure 7 is evaluated by using the DSM algorithm SCALE. In order to evaluated the DSM performance for a 10-user case and still holding the achievable data rate per user as a metric; Figures 11 and 12 represent two sections of the 10-dimensional rate region curve that isolates the relation between 2 arbitrary users, reducing then the graph to a 2-dimensional case. In Figure 11, the rate region for the NA channel measurement case and the corresponding confidence region are plotted for 2 users (out of 10 users) with nonequal length lines. Similarly, Figure 12 also shows the NA FEXT channel measurement case and the confidence region for 2 users, but for equal length lines (2200 m). Unlike the results shown in Section 7.1, both cases show
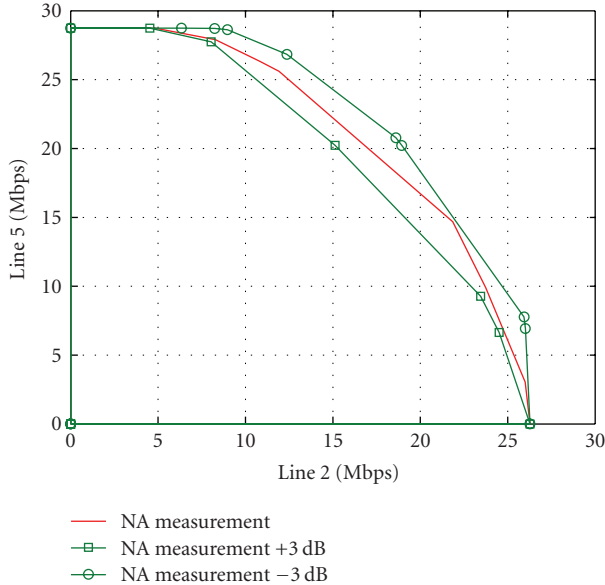
FIGURE 12: Section of the 10-dimensional rate region curve, obtained with SCALE, for 2 users (out of 10 users) with equal length lines (2200 m).

FIGURE 13: Total data throughput for the 10 users *Scenario II* using the SCALE algorithm, comprising approximately 100 profiles.

that some of the NA measurements border points are close to the confidence rate region limits. These fact arises from the nonlinear data rate relation between the users, that is dependent of, for example, different users priorities, channel states, and so forth. However, the data rates based on the NA measurements do not cross the confidence region limits.

Assuming now the total data throughput of *Scenario II* as a metric to evaluate the SCALE performance for this 10 users case, Figure 13 shows the total data rate for different profiles. In this work, the term profile stands for a predefined set of user priorities given to the DSM algorithms. In other words, by varying the users priorities, that is, defining different profiles, we provide a diversity of data rate combinations between the users. For a 2-users case, which comprises a two-dimensional rate region, this diversity corresponds to almost equally distributed (scattered points) along the rate region curves (border). The 10 users simulation using the ISB, comprising the same number of profiles (approximately 100 profiles), was skipped due to complexity issues, since it would required several days to be performed. However, it is believed that both ISB and SCALE presents similar performances, as indicated by the results for *Scenario I*.

In Figure 13, the total data rate values obtained by the SCALE, based on the NA measurements and the confidence rate region limits, are sorted separately in an ascending order, that is, the best/worst values of a curve are compared with the relative best/worst values of the other curves. The results in Figure 13 indicate that a variation of ±3 dB in the FEXT crosstalk channel estimates can result in a spread of the total data throughput of ±10 Mbps, for the specific 10 users scenario considered. On the other hand, this represents the extreme cases where all the crosstalk channel estimates for the 10 users, and for all the tones, assume an error $\widetilde{\Delta}_{dB} = \pm 3$ dB. Thus, we can interpret these extreme cases as limits for a total data throughput confidence region.

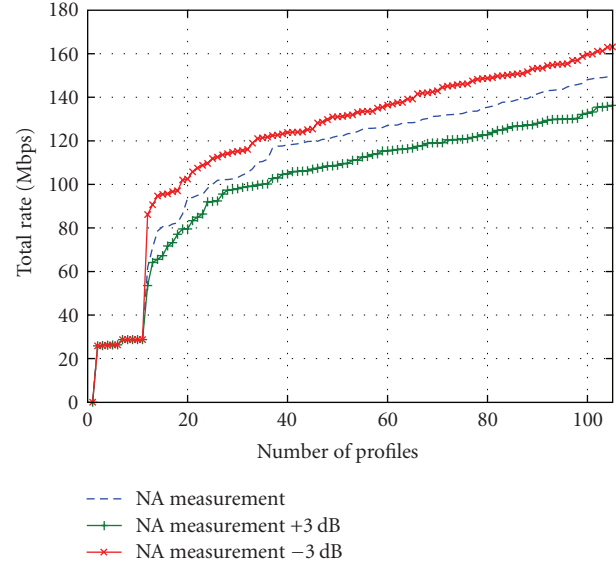## 8. Summary and Conclusions

The paper provides a statistical sensitivity analysis of the achievable bitloading assuming an uniformly distributed FEXT channel estimation error. The analysis comprises the derivation of the bitloading PDF and the data rate PDF resulting from the nonperfect FEXT channel estimation. The so-obtained data rate PDF is approximated by the Gaussian distribution with the use of the Central Limit Theorem. The validation of this approximation is numerically verified by comparing the derived PDF with the corresponding Monte Carlo simulations for measured FEXT channels of an ordinary twisted-pair cable. For the study case, a maximum spread of approximately 400 kbps in the data rate could be observed due to the FEXT channel estimation error. This corresponds to an uncertainty of less than 2% of the mean data rate for the considered line. Moreover, it could be noted that the data rate PDF becomes slightly biased when the background noise level is in the same range as the FEXT, in the sense that the mean data rate differs from the estimation error-free case. This is equivalent to a scenario that is also limited by the background noise, rather than just FEXT, whereas the assumed estimation error model is no longer valid.

The impact of the crosstalk channel estimation on the DSM performance was evaluated by means of computer simulations of the DSM algorithms ISB and SCALE. For the latter, measured channel information from different network scenarios, consisting of real twisted-pair cables, was used. From the achieved rate region curves, the following conclusions can be made. Using the worst-case FEXT model, the DSM performance is under-estimated compared to the one obtained with the *Crosstalk Estimator* [24], as expected. The ISB and SCALE algorithms achieved practically the same performance with both the *Crosstalk Estimator* and the

reference measurements. The results for the considered 10 users scenario applying the SCALE algorithm and assuming the total data throughput as a metric, indicate that the nonperfect FEXT channel estimates lead to a spread in the total data throughput of ± 10 Mbps, for the specific scenario considered. However, this should be considered as the extreme case, where all the crosstalk channel estimates for the 10 users, and for all the tones, assume an error-offset of ± 3 dB.

Acknowledgments

References

[1] T. Starr, J. M. Cioffi, and P. J. Silverman, *Understanding Digital Subscriber Line Technology*, Prentice-Hall, Upper Saddle River, NJ, USA, 1999.

[2] P. Golden, H. Dedieu, and K. Jacobsen, *Fundamentals of DSL Technology*, Auerbach Publications, Taylor & Francis, Boca Raton, Fla, USA, 2006.

[3] Dynamic Spectrum Management Technical Report, "ATIS committee NIPP pre-published document ATIS-PP-0600007," May 2007.

[4] K. B. Song, S. T. Chung, G. Ginis, and J. M. Cioffi, "Dynamic spectrum management for next-generation DSL systems," *IEEE Communications Magazine*, vol. 40, no. 10, pp. 101–109, 2002.

[5] T. Starr, M. Sorbara, J. M. Cioffi, and P. J. Silverman, *DSL Advances*, Prentice-Hall, Upper Saddle River, NJ, USA, 2003.

[6] R. Cendrillon, *Multi-user signal and spectra co-ordination for digital subscriber lines*, Ph.D. dissertation, Katholieke Universiteit Leuven, Leuven, Belgium, December 2004.

[7] J. Verlinden, T. Bostoen, and G. Ysebaert, "Dynamic spectrum management for digital subscriber lines—edition 2," Technology White Paper, Alcatel, June 2005.

[8] P. Golden, H. Dedieu, and K. Jacobsen, *Implementation and Applications of DSL Technology*, Auerbach Publications, Taylor & Francis, Boca Raton, Fla, USA, 2007.

[9] W. Yu, G. Ginis, and J. M. Cioffi, "Distributed multiuser power control for digital subscriber lines," *IEEE Journal on Selected Areas in Communications*, vol. 20, no. 5, pp. 1105–1115, 2002.

[10] R. Cendrillon and M. Moonen, "Iterative spectrum balancing for digital subscriber lines," in *IEEE International Conference on Communications (ICC '05)*, vol. 3, pp. 1937–1941, Seoul, South Korea, May 2005.

[11] R. Cendrillon, W. Yu, M. Moonen, J. Verlinden, and T. Bostoen, "Optimal multiuser spectrum balancing for digital subscriber lines," *IEEE Transactions on Communications*, vol. 54, no. 5, pp. 922–933, 2006.

[12] J. Papandriopoulos and J. S. Evans, "Low-complexity distributed algorithms for spectrum balancing in multi-user DSL networks," in *IEEE International Conference on Communications (ICC '06)*, vol. 7, pp. 3270–3275, Istanbul, Turkey, July 2006.

[13] D. Statovci, T. Nordström, and R. Nilsson, "Dynamic spectrum management for standardized VDSL," in *Proceedings of IEEE International Conference on Acoustics, Speech and Signal Processing (ICASSP '07)*, vol. 3, pp. 73–76, Honolulu, Hawaii, USA, April 2007.

[14] R. Cendrillon, J. Huang, M. Chiang, and M. Moonen, "Autonomous spectrum balancing for digital subscriber lines," *IEEE Transactions on Signal Processing*, vol. 55, no. 8, pp. 4241–4257, 2007.

[15] G. Ginis and J. M. Cioffi, "Vectored transmission for digital subscriber line systems," *IEEE Journal on Selected Areas in Communications*, vol. 20, no. 5, pp. 1085–1104, 2002.

[16] R. Cendrillon, G. Ginis, E. Van den Bogaert, and M. Moonen, "A near-optimal linear crosstalk canceler for upstream VDSL," *IEEE Transactions on Signal Processing*, vol. 54, no. 8, pp. 3136–3146, 2006.

[17] R. Cendrillon, G. Ginis, E. Van den Bogaert, and M. Moonen, "A near-optimal linear crosstalk precoder for downstream VDSL," *IEEE Transactions on Communications*, vol. 55, no. 5, pp. 860–863, 2007.

[18] J. W. Cook, R. H. Kirkby, M. G. Booth, K. T. Foster, D. E. A. Clarke, and G. Young, "The noise and crosstalk environment for ADSL and VDSL systems," *IEEE Communications Magazine*, vol. 37, no. 5, pp. 73–78, 1999.

[19] S. Galli, C. Valenti, and K. J. Kerpez, "A frequency-domain approach to crosstalk identification in xDSL systems," *IEEE Journal on Selected Areas in Communications*, vol. 19, no. 8, pp. 1497–1506, 2001.

[20] C. Zeng, C. Aldana, A. A. Salvekar, and J. M. Cioffi, "Crosstalk identification in xDSL systems," *IEEE Journal on Selected Areas in Communications*, vol. 19, no. 8, pp. 1488–1496, 2001.

[21] Y. Shi, F. Ding, and T. Chen, "Multirate crosstalk identification in xDSL systems," *IEEE Transactions on Communications*, vol. 54, no. 10, pp. 1878–1886, 2006.

[22] American National Standard for Telecommunications, "Spectrum Management for Loop Transmission Systems T1.417-2003, (issue 2)," 2003.

[23] ETSI, "Std. TS 101 270-1 v1.3.1. Transmission and multiplexing, access transmission systems on metallic access cables, very high speed digital subscriber lines (VDSL), part 1: functional requirements," July 2003.

[24] F. Lindqvist, N. Lindqvist, B. Dortschy, et al., "Crosstalk channel estimation via standardized two-port measurements," *EURASIP Journal on Advances in Signal Processing*, vol. 2008, Article ID 916865, 14 pages, 2008.

[25] M. Monteiro, N. Lindqvist, and A. Klautau, "Spectrum balancing algorithms for power minimization in DSL networks," in *IEEE International Conference on Communications (ICC '09)*, Dresden, Germany, June 2009.

[26] ITU-T Standard G.992.5, "Asymmetric digital subscriber line (ADSL) transceivers—extended bandwidth ADSL2 (ADSL2plus)," January 2005.

[27] A. Papoulis, *Probability Random Variables and Stochastic Process*, McGraw-Hill, New York, NY, USA, 3rd edition, 1991.